Composite Structures

Inclined composite guardrails/safety barriers – numerical and experimental evaluation of their transverse stiffnesses and compliance with standards

--Manuscript Draft--

Manuscript Number:	
Article Type:	Full Length Article
Keywords:	Composites; FE Analyses; Inclined Guardrails; Pultrusion; Testing; Tubes
Corresponding Author:	Geoffrey J. Turvey Lancaster University Lancaster, United Kingdom
First Author:	Geoffrey J. Turvey
Order of Authors:	Geoffrey J. Turvey
	Adam Sutch, MEng
Abstract:	Three-point flexure and axial torsion tests were undertaken to establish the longitudinal elastic flexural and in-plane shear moduli of pultruded GFRP tubes. They were used to define one-dimensional two-node beam elements for modelling single- and two-bay inclined guardrails with inclinations up to 60 o . Subsequently, three-dimensional FE models were developed to analyse more accurately single- and two-bay 30 o inclined guardrails. The results from these analyses were compared with those of full-scale load tests on 30 o inclined guardrails subjected to transverse normal preload, usability, and ultimate loads applied to the handrails. It is shown that the analysis results based one-dimensional elements significantly underestimate the mean handrail deflections and over-estimate the guardrails' transverse stiffness. By contrast, using three-dimensional elements in the FE models give more accurate predictions, with mean handrail deflections 9% and 14-16% lower than single- and two-bay test values respectively. The corresponding percentages for mean transverse stiffnesses are 10% and 12.5 – 14.3% higher respectively. It was also observed that the responses of the guardrails were linear, the residual deflections on unloading were less than permitted for the preload, usability and ultimate loads. Furthermore, neither the single- nor the two-bay 30 o inclined guardrails sustained any damage.
Suggested Reviewers:	

Cover Letter.docx

Engineering Department,
Lancaster University,
Gillow Avenue,
Bailrigg,
Lancaster,
LA1 4YW.

7th March 2021.

Professor A.J. Ferreira,
Editor,
Composite Structures,
Department of Engineering,
University of Porto,
Porto,
PORTUGAL.

Dear Professor Ferreira,

Title: Inclined composite guardrails/safety barriers – numerical and experimental evaluation of their transverse stiffnesses and compliance with standards

Authors: G.J. Turvey and A. Sutch

Please would you kindly arrange for our manuscript, referred to above, to be considered for possible publication in your journal, *Composite Structures*.

We look forward to receiving your decision on our manuscript's acceptability (or otherwise) for publication in *Composite Structures* in due course.

Yours sincerely,

G.J. Turvey

Inclined composite guardrails/safety barriers – numerical and experimental evaluation of their transverse stiffnesses and compliance with standards

G.J. Turvey [a] and A. Sutch [a,b]

[a] Engineering Department, Lancaster University, Gillow Avenue, Bailrigg, Lancaster, LA1 4YW, UK

[b] McLaren Automotive, McLaren Technology Centre, Chertsey Road, Woking, Surrey, GU21 4YH, UK

Abstract

Three-point flexure and axial torsion tests were undertaken to establish the longitudinal elastic flexural and in-plane shear moduli of pultruded GFRP tubes. They were used to define one-dimensional two-node beam elements for modelling single- and two-bay inclined guardrails with inclinations up to 60 °. Subsequently, three-dimensional FE models were developed to analyse more accurately single- and two-bay 30 ° inclined guardrails. The results from these analyses were compared with those of full-scale load tests on 30 ° inclined guardrails subjected to transverse normal preload, usability, and ultimate loads applied to the handrails. It is shown that the analysis results based one-dimensional elements significantly underestimate the mean handrail deflections and over-estimate the guardrails' transverse stiffness. By contrast, using three-dimensional elements in the FE models give more accurate predictions, with mean handrail deflections 9% and 14-16% lower than single- and two-bay test values respectively. The corresponding percentages for mean transverse stiffnesses are 10% and 12.5 – 14.3% higher respectively. It was also observed that the responses of the guardrails were linear, the residual deflections on unloading were less than permitted for the preload, usability and ultimate loads. Furthermore, neither the single- nor the two-bay 30 ° inclined guardrails sustained any damage.

Keywords: Composites, FE Analyses, Inclined Guardrails, Pultrusion, Testing, Tubes

1. Introduction

Guardrails are used to prevent single/multiple individuals from falling off raised platforms, walkways, balconies and staircases and sustaining life-threatening injuries or even death. The guardrails are constructed from natural materials such as bamboo and timber as well as metallic materials such as wrought/cast iron, steel and aluminium.

About three decades ago interest started to develop in the possible use of composite materials in guardrails [1]. In particular, the use of glass fibre reinforced polymer (GFRP) composite tubes of circular and square cross-section were foreseen as possible superior alternatives for the posts, handrails and kneerails of the low load capacity timber and metallic guardrails. An important driver of this perception was the fact that the GFRP tubes are manufactured economically by pultrusion [2]. They are also more durable than metallic tubes and require less maintenance. In addition, GFRP guardrails are significantly lighter than metallic guardrails, more economical to transport to site and easier to handle on site and can be assembled using simple hand tools.

Nowadays, GFRP guardrails are often seen around the periphery of multi-story buildings under construction and around the edges of offshore platforms where their low self-weight, corrosion resistance and their electrical/thermal insulating properties are advantageous.

Although the use of GFRP guardrails, particularly modular guardrails, has increased substantially over the past decade, their structural performance has not been the subject of intensive research, most probably because they are regarded as secondary structures and so they do not attract the same level of kudos as research on aerospace structures. Unsurprisingly therefore, although load test reports (see [3] – [6]) on guardrails have been provided to manufacturers and suppliers of modular guardrails, it is only relatively recently that serious research on these structures has been undertaken (see [7] - [10]). Furthermore, all of the latter investigations have focused on horizontal guardrails. It is believed that the present paper is the first to present a research investigation on inclined modular guardrails.

2. Elastic Properties of Guardrail Tubes

Pultruded GFRP composite circular cross-section tubes are commonly used for the posts and rails in guardrails. In the present investigation the tubes have a nominal outside diameter of 50 mm and wall thickness of 5 mm. From the standpoint of design/structural analysis, the important material properties of the GFRP tubes are their elastic flexural and shear moduli. These properties are determined by simple mechanical testing. Three point flexure tests are used to determine the elastic flexural modulus. A length of tube is selected and four straight lines are drawn along its outer surface parallel to its axis. The lines are spaced at 90^o intervals around the surface and their ends are labelled A, B, C and D respectively. A further two circumferential lines 1400 mm apart are drawn around the tube's circumference and normal to its axis. The latter lines define the positions of the simple supports in the symmetric three-point flexure tests on the tube.

In the present investigation, 12 load – unload tests were carried out on the 1400 mm span tube, i.e. three repeat tests with the lines A-A, B-B, C-C and D-D uppermost in turn. During each test the mid-span loads and deflections were recorded. The maximum load was approximately 795 N and the mid-span deflections ranged from 7.34 mm to 7.55 mm. Load versus mid-span deflection responses were plotted and proved to be linear for each tube orientation. After completing the tests, the tube was shortened to a span of 800 mm and a further 12 load – unload tests were carried out. In these tests the maximum applied load was approximately 1089 N and the mid-span deflections ranged from 2.11 mm to 2.36 mm. Again, the load versus mid-span deflection responses were linear.

Particular load and deflection values, taken from the mean linear responses of the 1400 mm and 800 mm flexure tests, were combined with the second moment of area of the tube's cross-section, to determine two sets of four values of elastic flexural modulus with respect to each of the lines A-A – D-D. The individual, mean and overall mean elastic flexural moduli are given in Table 1.

Insert Table 1

The elastic shear modulus of the pultruded GFRP circular cross-section tube was determined by carrying out axial torsion tests on three lengths of tube, i.e. 200 mm, 400 mm and 600 mm in a torsion test rig. For the 600 mm torsion test the tube was cut to a length of 670 mm to accommodate a 35 mm long joint for a metal plug bonded into each tube end. The plug at one

end of the tube was connected to a wheel which could be rotated manually to apply a measured axial twist to that end of the tube. The plug at the other end of the tube was fixed to the centre of a horizontal bar normal to the tube's axis. A spirit level was positioned along the bar with its transverse centreline aligned with the tube's axis. A calibrated spring balance at a known distance from the bar's axis recorded the vertical load (and hence the torque on the tube) when the spirit level was horizontal. Two straight lines 180^o apart were drawn along the tube's outer surface parallel to its axis. Two uniaxial strain gauges were bonded to the tube's surface at the mid-length of each line. The sensitive axes of the gauges were oriented at +45^o and -45^o to the line in order to measure the shear strain during the torsion test. The 600 mm tube was torqued incrementally up to a torque of 30 Nm before unloading incrementally to zero torque. The maximum twist was 19.2^o. The test was repeated a further two times. The torque – twist responses were linear and repeatable. The tube was then removed from the torsion test rig and the end plug regions of the tube were cut off and heated to allow the plugs to be removed. The tube was then shortened to 475 mm and the process of bonding in the end plugs and testing the shortened tube was repeated three times. After completing the third test, the plugs were again removed and the tube was shortened to 275 mm and retested. All of the torque - twist responses of the 400 mm and 200 mm tubes were linear and repeatable. The test data were then processed to determine the individual, mean and overall mean shear moduli of the tubes, as shown in Table 2.

Insert Table 2

3. Inclined Guardrail Geometry

An image of an inclined two-bay guardrail is shown in Figure 1. The guardrail has three vertical members, usually referred to as posts, and two inclined members. The upper inclined member is referred to as the handrail and the lower inclined member is referred to as the kneerail. In the present modular guardrails all three types of member (posts, handrail and kneerail) are 50 mm diameter circular cross-section pultruded GFRP tubes with 5 mm wall thicknesses.

There are several design standards relevant to modular guardrails (see [11] & [12]). In these standards guidance is given for the post spacing and the overall height of the handrail and the distance between the kneerail and the ground. However, this design guidance is given for a horizontal guardrail. Apart from specifying the maximum normal centreline distances between the handrail and the kneerail as 500 mm and the knee rail and the inclined surface also as 500 mm, the only other dimension is the spacing between the vertical posts, which must not exceed 1500 mm. As drawn in Figure 1, the spacing between the vertical posts is 1250 mm and the distance of the top of the kneerail above the post base is 550 mm and the top of the handrail is 1100 mm above the post base.

The angle of inclination θ of the slope on which the post bases of the inclined guardrail are fixed is also shown in Figure 1. In the initial Finite Element (FE) analyses, the effects of five guardrail inclinations, i.e. $\theta = 0^o$, 15^o, 30^o, 45^o and 60^o, on their transverse deformations and stiffnesses are investigated. However, in the later sections the results of a more detailed FE analysis for a slope of 30^o will be compared with results of several load tests on single- and two-bay guardrails on 30^o slopes.

Insert Figure 1

In guardrails the joints between posts and rails are formed by bolted two-part moulded GFRP connectors. Thus, two-way connectors are used to join the tops of the outer posts to the handrail. Similarly, a three-way connector is used to join the top of the middle post to the handrail. The same type of connector is used to join the outer ends of the kneerails to the outer posts. And last, but not least, the four-way connector is used to join the interior ends of the kneerails to the middle post. Images of these connectors are shown in Figure 2.

Insert Figure 2

Two types of base are used to connect the guardrails' posts to the inclined surface, namely *Foot* and *Side-fit* bases which are illustrated in Figure 3. However, in the FE analyses presented later only Foot bases are considered.

Insert Figure 3

4. Finite Element Analyses of Single- and Two-Bay Guardrails

4.1 ANSYS Mechanical APDL Analysis

The results from the simpler of the two ANSYS Finite Element (FE) analyses of guardrails are presented first. The analysis is used to calculate the transverse deflections of the handrail and the overall transverse stiffnesses of single- and two-bay guardrails when loads act normal to the plane of the guardrails at the tops of the posts and the mid-spans of the handrails. These quantities are determined for a range of inclinations θ. Although the design codes for guardrails specify load tests on two-bay guardrails for serviceability and ultimate load compliance, single-bay guardrails are also analysed for comparison purposes.

Sketches of single- and two-bay guardrail models for the FE analyses are presented for an arbitrary slope angle θ, as shown in Figures 4 and 5 respectively. In Figure 4 the numbers 3, 4, 5 and 6 are the nodes of the FE model at the joints between the posts and rails. Likewise, the numbers 1 and 2 are the nodes between the post bases and the inclined surface, and number 7 is the node at the centre of the handrail.

Insert Figure 4

Similarly, Figure 5 shows the FE model of an inclined two-bay guardrail with the numbers 4 – 9 representing the nodes in the FE model at the joints between the posts and rails. Likewise, the numbers 1 – 3 represent the nodes between the post bases and the inclined surface, and 8(0) and 8(1) represent the nodes at the centres of the lower and upper lengths of the handrail.

Insert Figure 5

In both guardrail models the joints between the posts and rails are assumed rigid, whereas the post base joints are assumed to be revolute joints with a single plane of rotation normal to the plane of the guardrail. These joints are assumed to have the same mean rotational stiffness of 116 kNm/rad. Further details of the cantilever tests used to determine this mean stiffness are given in [10].

The single-bay guardrail results with the ultimate load $F_u = 697N$ applied at the mid-span of the handrail (Node 7 in Figure 4) are presented first. The load is greater than the ultimate load

given in [11]. It equals the maximum load in the guardrail tests described later. Five single-bay guardrails are analysed for $\theta = 0^o, 15^o, 30^o, 45^o$ and 60^o. The transverse nodal deflections are given in Table 3 together with the transverse stiffnesses, calculated using Eq,(1a):-

$$K_T^1 = \frac{3F_u}{\left(\delta_5 + \delta_6 + \delta_7\right)} \tag{1a}$$

In Eq.(1a) K_T^1 is the transverse stiffness of the single-bay inclined guardrail and δ_5, δ_6 and δ_7 are the transverse deflections of the tops of the lower and upper posts and the mid-span of the handrail respectively for each particular inclination θ.

Insert Table 3

It is evident from Table 3 that the transverse stiffness of the guardrail increases approximately linearly by about 5.8% as the inclination increases to 60^o. On the other hand, the mid-span deflection of the handrail increases nonlinearly for $\theta \geq 30^o$. Indeed, at $\theta = 60^o$, the mid-span deflection is 37% greater than the mid-span deflection when $\theta = 0^o$.

Similar results have been computed for the two-bay guardrail for transverse loads of 697 N applied in turn at the top of the centre post (Node 8) and at the mid-spans of the handrail, i.e. Nodes 8(0) and 8(1). The handrail deflections corresponding to the three loading points and the transverse stiffness are presented in Table 4.

The transverse stiffnesses of the two-bay guardrails are calculated from Eq,(1b):-

$$K_T^2 = \frac{5F_u}{\left(\delta_7 + \delta_8 + \delta_9 + \delta_{8(0)} + \delta_{8(1)}\right)} \tag{1b}$$

In Eq.(1b) K_T^2 is the transverse stiffness of the two-bay inclined guardrail and δ_7, δ_8 and δ_9 are the transverse deflections of the tops of the lower, centre and upper posts, and $\delta_{8(0)}$ and $\delta_{8(1)}$ are the transverse deflections of the lower and upper mid-spans of the handrail respectively for each particular inclination θ.

Insert Table 4

4.2 ANSYS Workbench Analysis

Following the simple one-dimensional FE analyses of the one- and two-bay guardrails for a range of inclinations, it was decided to create a three-dimensional model of the two guardrails for a $\theta = 30^o$ inclination. This inclination was chosen to correspond to the physical tests on guardrails, described in the next section.

In order to develop three-dimensional FE analyses of the one- and two-bay guardrails, three-dimensional elastic moduli were needed, as the test work described in Section 2 only provided values for the tubes' longitudinal elastic modulus and in-plane shear modulus. However, it was deemed impractical to engage in extensive trial and error, iterative analyses to determine accurate values for the other *unknown* elastic and shear moduli. Therefore, they were assumed to be 0.7 times the longitudinal elastic and in-plane shear moduli, respectively. Furthermore, it

was anticipated that the values of the unknown Poisson's ratios would not significantly affect the analysis results and so values of 0.3 were used.

Three-dimensional models of the one- and two-bay guardrails with 30^o inclines were created using Solidworks [13]. Several features were introduced into the models to ensure their compatibility and ease of use. For example, small solid cylindrical extrusions were added at particular loading points on the tubes. These features enabled loads to be added by selecting the extrusions' end faces. Furthermore, sharp and/or zero thickness zones were eliminated in order to avoid FE meshing problems. Having, resolved these potential issues the Solidworks models were imported into ANSYS for meshing, followed by applying the loads and constraints (zero displacements in three mutually orthogonal directions at the bottom surfaces of the post bases) and specifying the output responses of interest, e.g. deflections at the tops of the posts and the mid-spans of the handrails.

Nodal deflections are presented in Table 5 for the single-bay guardrail when horizontal loads of $F_s = 350N$ and $F_u = 697N$ respectively are applied in turn at the mid-span of the handrail normal to the plane of the guardrail. These loads correspond approximately to the *usability* and *strength* loads for the guardrail given in [12]. Also given in Table 5 are the transverse stiffnesses of the guardrail, calculated using Eq.(1a).

Insert Table 5

Comparing Tables 3 and 5, it is evident that under a load of $697N$ applied at Node 7 the handrail deflections are larger in the three-dimensional model of the guardrail. Also, the three-dimensional model shows that the top of the lower post deflects about 10.7% more than the upper post.

The results obtained from the three-dimensional FE analysis of the two-bay 30^o inclined guardrail with $350N$ and $697N$ loads applied at the mid-spans of the handrail and the top of the centre post are given in Table 6.

Insert Table 6

It is evident that the deflections obtained for the maximum loads applied at the mid-spans of the handrails are larger for the three-dimensional model analyses than for the one-dimensional model analyses (cf. Tables 4 and 6).

The mean transverse stiffness for the single-bay guardrail with a 30^o incline is $17.05kNm^{-1}$, i.e. approximately 30% lower than the transverse stiffness calculated using the simpler FE analysis. Likewise, the mean transverse stiffness of the two-bay guardrail with a 30^o incline is $26.15kNm^{-1}$ which is considerably lower than that calculated using the simpler FE analysis. Despite their lower stiffnesses both guardrails comply with the deflection limits given in [11] and [12].

5. Experimental Tests on 30º Inclined Single- and Two-Bay Guardrails

5.1 Assembly of the Guardrails on the Laboratory Strong Floor

In order to provide transverse deflection and stiffness data for comparison with the three-dimensional FE analysis data and, in so doing, establish its accuracy and utility, it was decided to fabricate two pultruded GFRP modular guardrails with 30^o inclines. Furthermore, it was felt that instead of using two-way connectors to form the joints between the tops of the end posts and the handrails, it would be more efficient to use three-way connectors. In addition, it was decided to fabricate and test the two-bay guardrail with a 30^o incline first. These choices made it easier to reduce the two-bay guardrail to a single-bay guardrail for the second stage of testing. Thus, only two types of connector were used in both the single- and two-bay 30^o inclined guardrails.

The guardrails were to be tested in the Engineering Department's Structures Laboratory. As the two-bay guardrail was tested first, the *giant meccano* steel work was used to form three rigid steel supports bolted to laboratory strong floor. Each support included a rigid steel angle, the top surface of which was at the required elevation for bolting each post foot base of the guardrail to achieve its required 30^o incline. Figure 6 shows the two-bay guardrail set up on the strong floor.

Insert Figure 6

After completing the load tests on the two-bay guardrail with a 30^o incline, the single-bay version of the guardrail was formed by removing the upper post and the upper kneerail. The four-way connector at the upper end of the lower kneerail was replaced with a three-way connector. Finally, the upper length of the handrail was removed. The resulting single-bay guardrail with a 30^o incline is shown bolted to its supports in Figure 7.

Insert Figure 7

5.2 Load Testing of the Guardrails

The load testing of the single- and two-bay inclined guardrails was carried out in accordance with the procedures set out in [12]. Cables were attached in turn at the mid-bay positions of the handrails and the top of the centre post (two-bay guardrail only). Figure 8 shows the loading cable attached to the mid-bay position. Also shown in Figure 8 is the tip of a dial gauge in contact with a small metal plate bonded to the mid-span of the handrail to record the transverse deflection of the handrail as the load in the cable increases.

Insert Figure 8

The tensile force acting horizontally and normal to the plane of the guardrail is produced by the steel cable supporting slotted steel disks of mass $10kg$ on a hanger. The cable runs horizontally from the handrail over a pulley wheel and then vertically to a load hanger at its end. The pulley wheel is supported by a rigid post attached to the laboratory strong floor, as shown in Figure 9.

Insert Figure 9

The test standard for guardrails [12] defines three load and deflection criteria that two-bay horizontal guardrails have to comply with. They are referred to as: (1) a pre-load F_p which is

designed to eliminate bedding-in effects after initial unloading, (2) a usability load F_u for normal operating effects which must not exceed a deflection of 30 mm and (3) a strength load F_s, corresponding to the maximum applied load, for which the deflection after unloading must not exceed 3.75 mm. Even though these loads are specified as acting normal to the plane of two-bay guardrails with $\theta = 0^o$, they will be used for the present guardrails with 30^o inclines. The forces F_p etc. are defined according to Eqs. (2) – (4):-

$$F_p = 75x1.25N = 94N \tag{2}$$

$$F_u = 300x1.25N = 375N \tag{3}$$

$$F_s = 1.75xF_u = 1.75x375 = 656N \tag{4}$$

However, in the load tests on the single- and two-bay guardrails with 30^o inclines it was not possible to apply these loads exactly using masses in the form of $10kg$ slotted steel disks. Hence, the test load used for the usability state was $350N$, i.e. about 7% lower than required. Similarly, the test load for the strength state was $697N$, i.e. about 6% greater than required.

The two-bay inclined guardrail was tested first. The top of the centre post and the mid-spans of the upper and lower handrails were loaded incrementally in turn up to the maximum load of $697N$ and then unloaded decrementally to zero load. This load – unload procedure was repeated three times. The deflections of the top of the centre post and the mid-spans of the upper and lower handrails were recorded for each load increment/decrement. Plots of load versus deflection during the third loading phase when the load was applied at the top of the centre post are shown in Figure 10. It is evident that the response is linear in all cases and that the deflections at the upper post and upper handrail mid-span are slightly larger than their corresponding lower post and lower handrail mid-span deflections. Although the unloading data points are not shown in Figure 10, there was no significant evidence of hysteresis in the responses, and the residual deflections ranged from $1-2mm$, i.e. less than the $3.75mm$ allowed.

Although not shown here, the maximum deflection was when the load of $697N$ was applied at the upper mid-span of the handrail and amounted to about $45mm$ and at a load of $350N$ it was about $22.5mm$.

The mean transverse stiffness obtained from all of the tests on the two-bay 30^o inclined guardrail was $22.65kNm^{-1}$. This is about 12% lower than the value predicted by ANSYS workbench.

Insert Figure 10

Similar data have been obtained from three repeat load – unload tests on the single-bay 30^o inclined guardrail with the maximum load of $697N$ applied at the mid-span of the handrail. The test data of the third repeat test are plotted in Figure 11.

Insert Figure 11

At the maximum load of $697N$ the maximum deflection was about $49mm$. This was slightly larger than that of the two-bay guardrail, thereby suggesting that its transverse stiffness was lower. Likewise, the data for Node 7 indicates that at a load of $350N$, the deflection is about $25mm$, which is within the $30mm$ limit for the F_u load. For the single-bay guardrail, there was negligible hysteresis and minimal residual deflection on unloading.

The overall mean transverse stiffness of the single-bay 30^o guardrail was calculated as $16.02kNm^{-1}$ which is within 6% of the value predicted by the ANSYS Workbench analysis.

6 Comparison of Numerical and Experimental Deflections and Transverse Stiffnesses of Guardrails

6.1 Working Loads (350N) on Single and Two-Bay 30º Inclined Guardrails

The results comparison for these two cases are presented in Tables 7 and 8 respectively. In Table 7 it is evident that the numerical and experimental mean handrail deflections are in reasonable agreement and that the numerical mean transverse stiffness over-estimates the experimental transverse stiffness by about 8.8%.

Insert Table 7

Insert Table 8

In Table 8 it is evident that the ANSYS Workbench analyses over-estimate the experimentally determined transverse stiffnesses of the two-bay 30^o inclined guardrails by between $14-17\%$. Furthermore, it is also evident that the mean experimental transverse stiffness of the two-bay 30^o inclined guardrail is $22.23kNm^{-1}$, i.e. about 31% greater than the corresponding single-bay guardrail. The mean two-bay guardrail deflection is 15.75 mm compared to 22.47 mm for the single-bay guardrail.

6.2 Ultimate Loads (697N) on Single- and Two-Bay 30º Inclined Guardrails

For these deflection and transverse stiffness comparisons ANSYS Mechanical APDL results are also included. In Table 9 the mean deflections and transverse stiffnesses obtained for the two numerical analyses of the 30^o single-bay guardrail are compared with the experimental values for the case of the ultimate load of $697N$ applied at the mid-bay of the handrail.

Insert Table 9

It is evident that the ANSYS Mechanical APDL analysis under-predicts the mean handrail deflection by about 37% and over-predicts the transverse stiffness by about 58%. By contrast the ANSYS Workbench analysis is significantly more accurate; under-estimating the mean handrail deflection by 9% and over-estimating the mean transverse stiffness by 10.1%.

Similar comparisons for mean handrail deflection and mean transverse stiffness are presented in Table 10 for the two-bay 30^o inclined guardrail. However, three loading situations are considered, namely the ultimate load of $697N$ applied in turn at the top of the centre post and at the lower and upper mid-spans of the handrail.

Again, it is clear that the ANSYS Mechanical APDL analysis significantly under-estimates the mean handrail deflections by $37-38\%$ and over-estimates the transverse stiffness by $59-61\%$ It is self-evident from Table 10 that the ANSYS Workbench analysis provides much better estimates of the experimental results. The mean handrail deflections being $10.8-12.5\%$ lower than the mean handrail deflections and the mean transverse stiffness being $12.5-14.3\%$ higher than the experimental mean transverse stiffnesses.

Finally, it is worth pointing out that the experimental one- and two-bay 30^0 inclined guardrail were able to support the loads without any evidence of damage. Their load versus deflection responses were linear and repeatable and residual deflections were of the order of $1-2mm$, i.e. within the $3.75mm$ limit prescribed in [11] and [12].

Insert Table 10

7. Concluding Comments

It is believed that the FE analyses and the load tests of single- and two-bay inclined pultruded GFRP composite modular guardrails are the first of their type to be reported.

The ANSYS Mechanical APDL software was used to analyse single- and two-bay guardrails with inclinations ranging from 0^o-60^o using two-node, one-dimensional, six degree of freedom finite elements. These analyses reported mean handrail deflections and transverse stiffnesses for the ultimate load of $697N$. For the single-bay guardrails there was about a 6% reduction in mean handrail deflection at an inclination of 60^o compared to the 0^o inclination. This corresponded to a 5.8% increase in transverse stiffness over the same angular range. However, for the two-bay inclined guardrails, the reduction in mean handrail deflection over the same angular range was about 14% and for the transverse stiffness the increase was 31.3% Furthermore, the transverse stiffnesses of the two-bay guardrails were about 44% (for 0^o inclination) and 78% (for 60^o inclination) larger than the transverse stiffnesses of the single-bay guardrails.

The ANSYS Workbench FE software was used to carry out three-dimensional analyses of single- and two-bay 30^o inclined guardrails. The mean handrail deflection and transverse stiffness data obtained was compared with corresponding data from tests on pultruded GFRP composite modular guardrails. These comparisons were made for the approximate usability and ultimate loads of $350N$ and $697N$. The most obvious conclusion from these comparisons was that the use of three-dimensional elements in the FE analyses produced significantly more accurate results for both load cases. Thus, for the approximate usability situation the transverse stiffness of the single-bay guardrail was approximately 9% higher than the test value and for the two-bay guardrail it was between 14% and 16% higher. The corresponding percentages for the transverse stiffnesses for the ultimate loads were 10% (single-bay) and 12.5% to 14.3% (two-bay).

Finally, it should be appreciated that the load – deflection response was essentially linear in the single- and two-bay load tests up to the ultimate load. Furthermore, each test was repeated three times and there was no evidence of any significant hysteresis and the residual deflections were less than $3.75mm$. Likewise, the maximum deflections at the usability and ultimate loads were all less than the values specified in [11] and [12],

8. Acknowledgements

The Authors wish to express their appreciation of the help and assistance provided by the Engineering Department's technician staff with the computational and experimental aspects of this research investigation.

Data Availability

The raw/processed data required to reproduce these findings cannot be shared at this time due to technical and time limitations.

9. References

1. Turvey GJ and Slater RC. Tests on pultruded GRP posts for handrail/barrier structures. 1st International Conference on Advanced Composite Materials in Bridges and Structures, Sherbrooke, 7th-9th October 1992. Published in Advanced Composite Materials in Bridges and Structures, Edited by K.W. Neale and P. Labossiere, Canadian Society for Civil Engineering, (1992), 319-329.

2. Anon. EXTREN Design Manual, Bristol Virginia, USA: Strongwell,1989.

3. Slater RC, Turvey GJ. Tests on GRP posts and handrailing system. Lancaster University Engineering Department Report; 1991.

4. Turvey GJ. Report on pultruded GRP post and handrail tests. Lancaster University Engineering Department Report; 2003.

5. Turvey GJ and Salisbury M. Tests on pultruded post and rail safety barriers, Lancaster University Engineering Department Report LU02011, 10th October 2012.

6. Turvey GJ. An experimental investigation of the serviceability, ultimate and failure loads of pultruded GFRP tubular posts with bolted composite bases, Lancaster University Engineering Department Report No.2018-1, November 2018, pp.13.

7. Turvey G. Experimental investigation of the load-deformation behaviour of pultruded GFRP modular and custom safety barriers. Composite Structures 2015;133:659-66.

8. Manalo A, Jackson M. Behaviour of pultruded glass fibre reinforced composites guardrails system. Advanced Structural Engineering 2018;21(4):545-56.

9. Manalo A, Pac M. Structural behaviour of pultruded fibre composites guardrail system under horizontal loading. Proceedings of the Institution of Mechanical Engineers 2018;232(4):273-86.

10. Turvey GJ, Milburn J, Two-bay pultruded GFRP safety barrier/guardrail – testing, analysis and compliance with standards. Composite Structures 253 (2020): 112745, 1-12.

11. BS 4592-0:2006, Flooring, stair treads and handrails for industrial use. British Standards Institution, London, 2006.

12. ISO 14122-3:2001, Safety of machinery – permanent means of access to machinery – Part 3: Stairways, stepladders and guardrails, 2001.

13. https://www.solidworks.com.

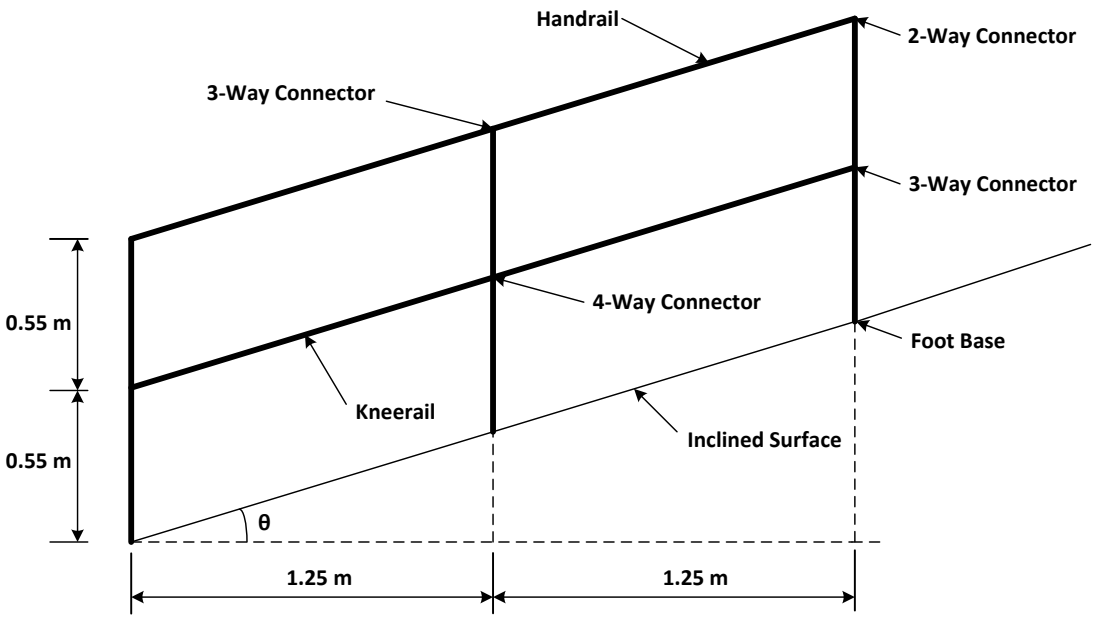
Handrail
2-Way Connector
3-Way Connector
3-Way Connector
4-Way Connector
Foot Base
0.55 m
Kneerail
0.55 m
Inclined Surface
θ
1.25 m
1.25 m

Figure 1

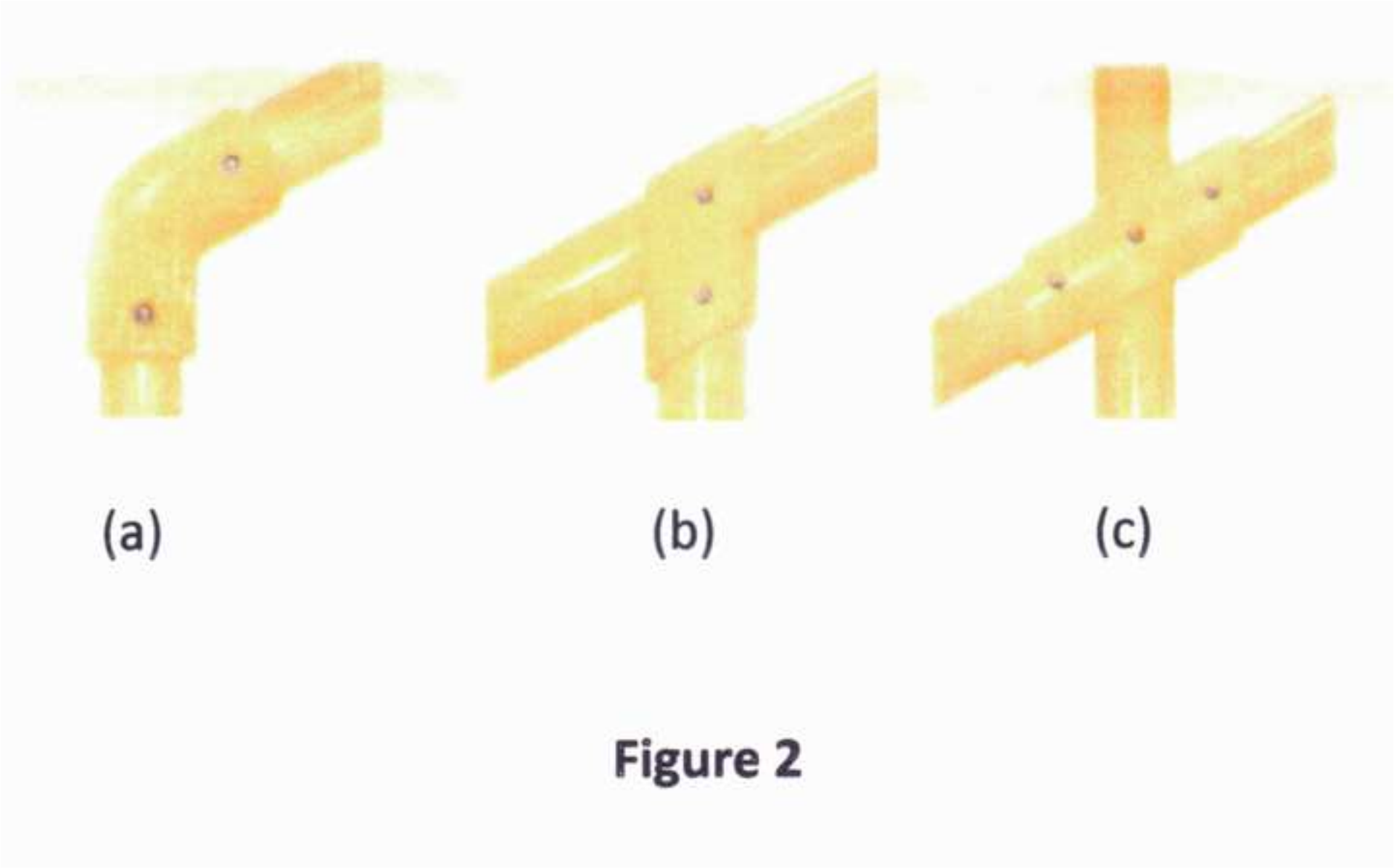

Figure 2

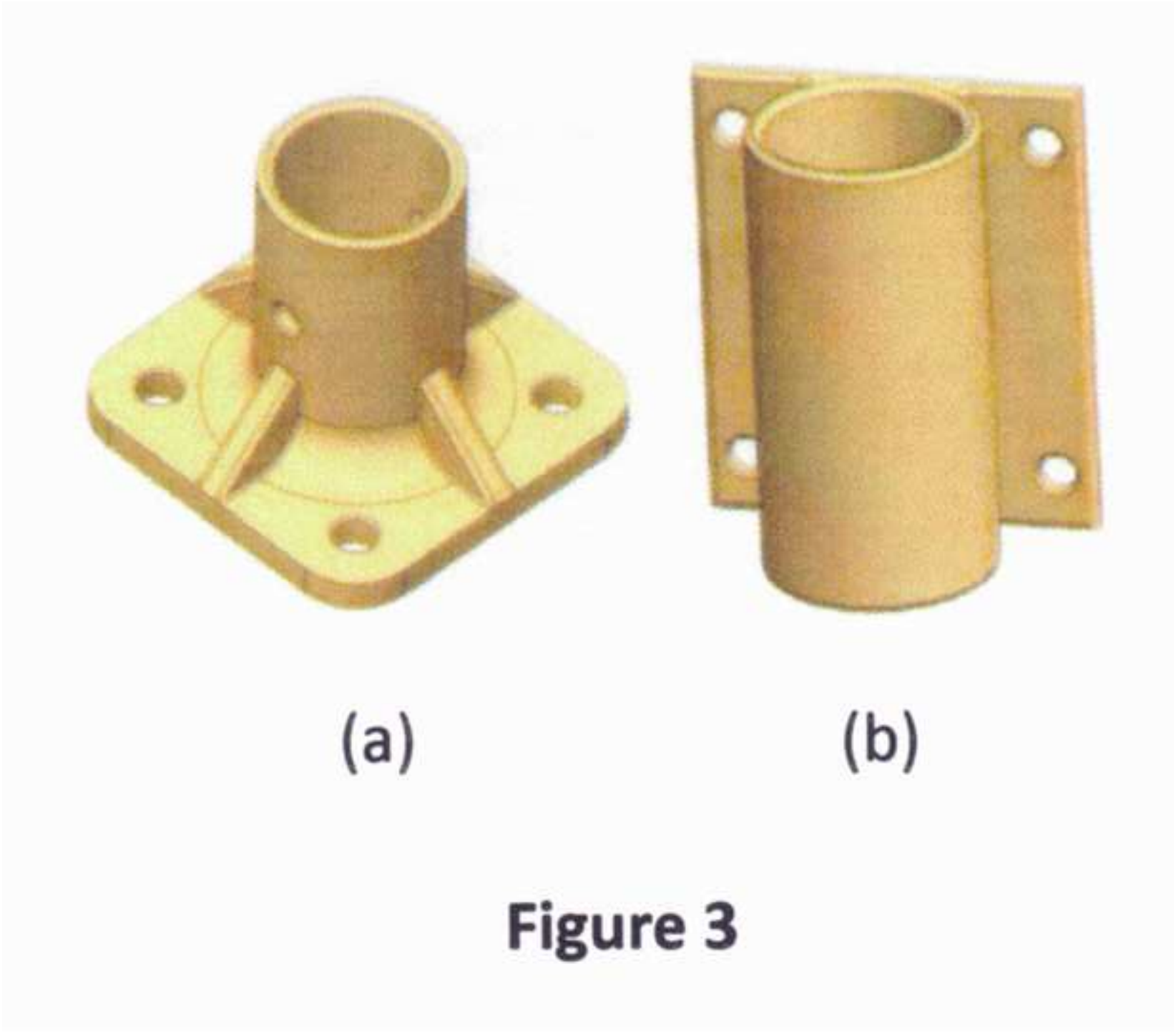

Figure 3

Figure 4

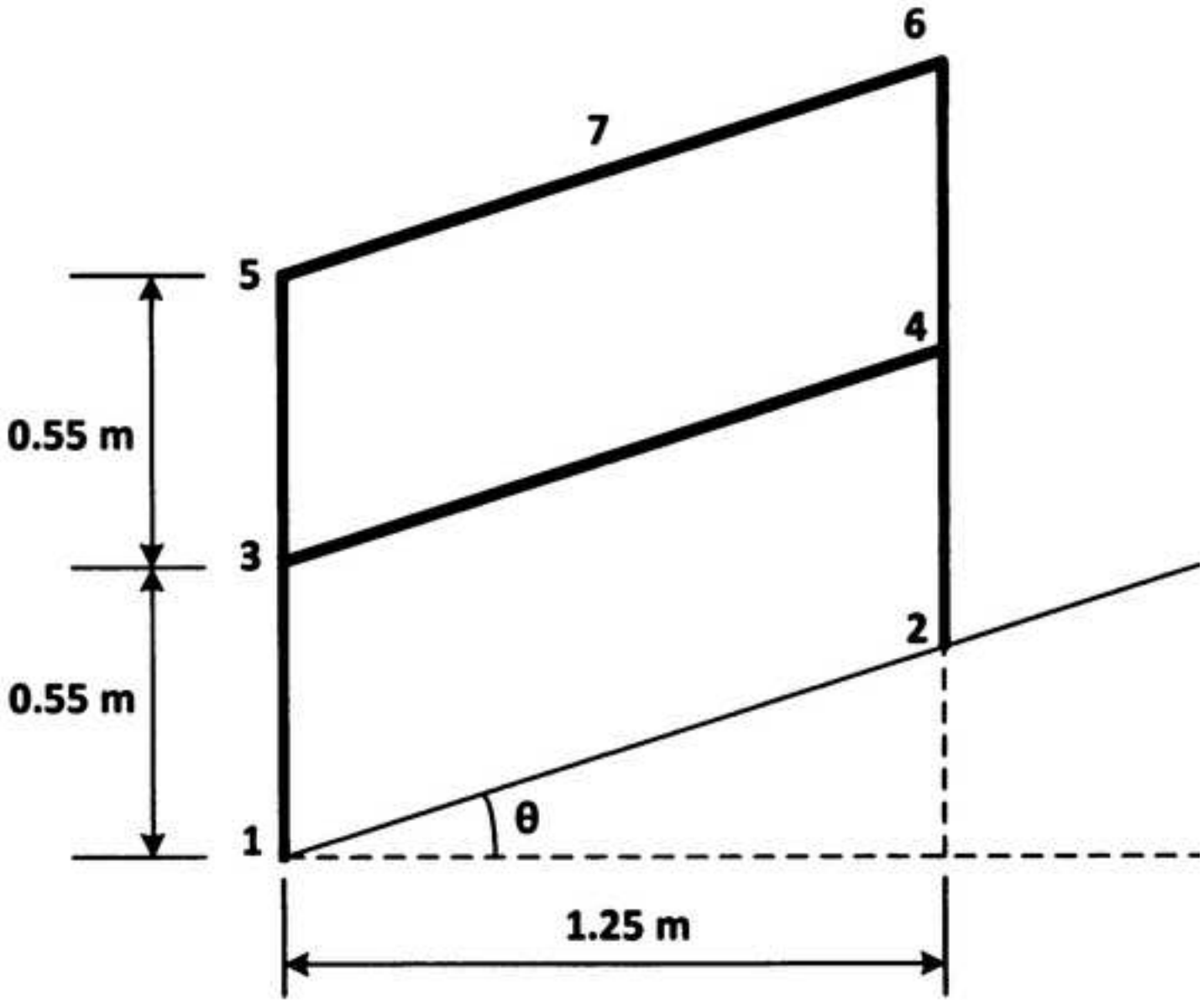

Figure 4

Figure 5

Click here to access/download;Figure;Figure 5 001.tif

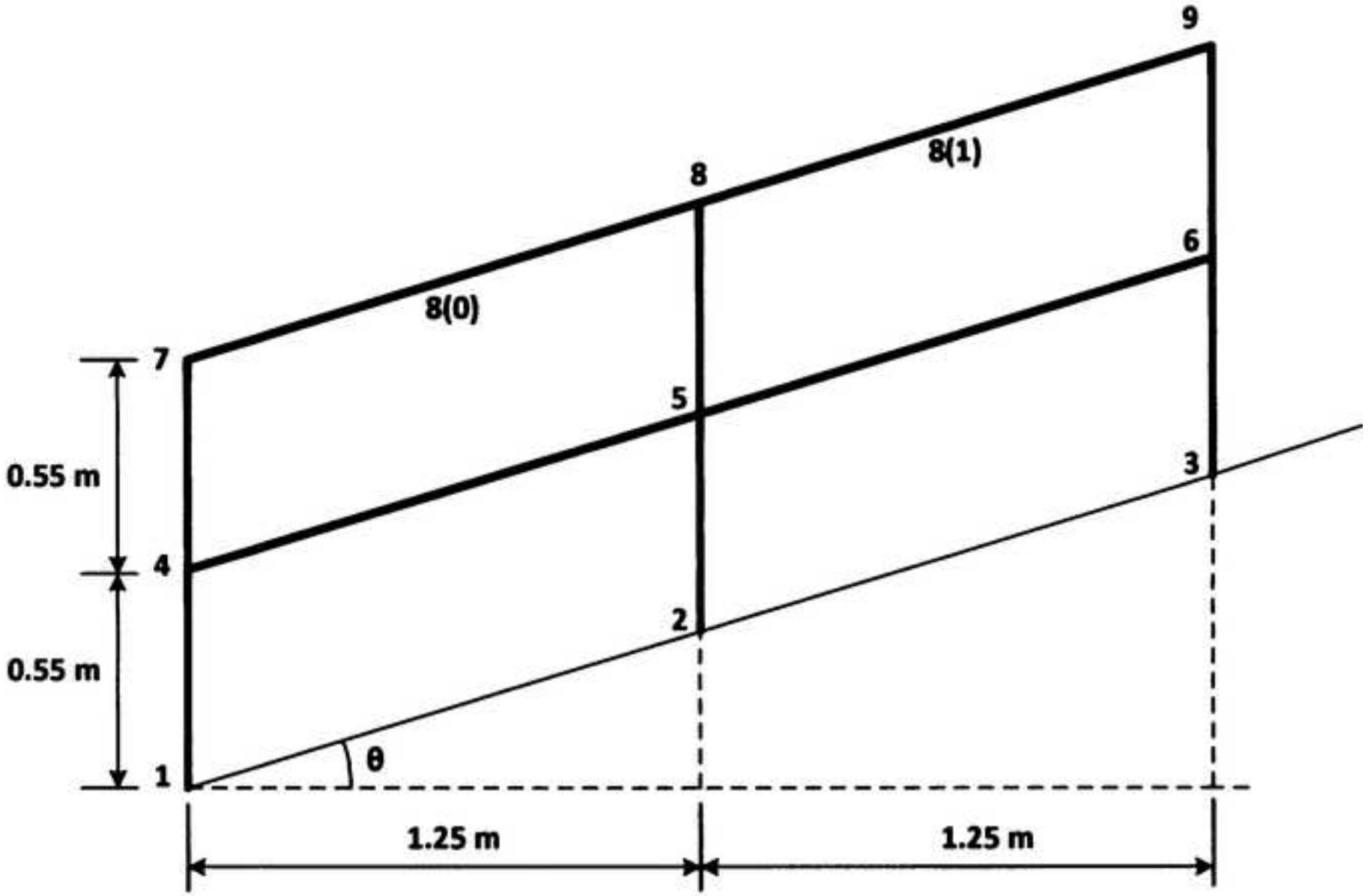

Figure 5

Figure 6

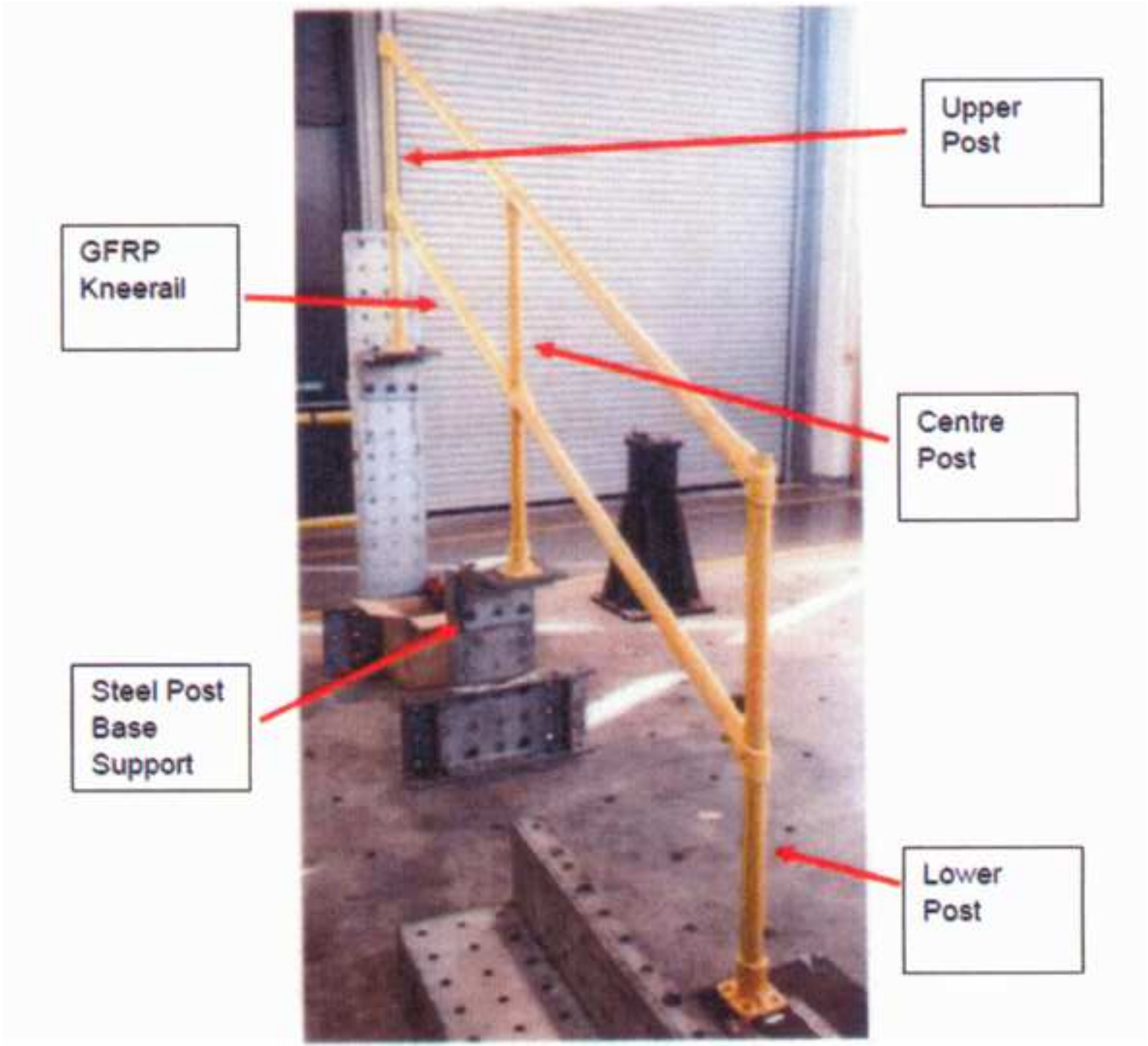

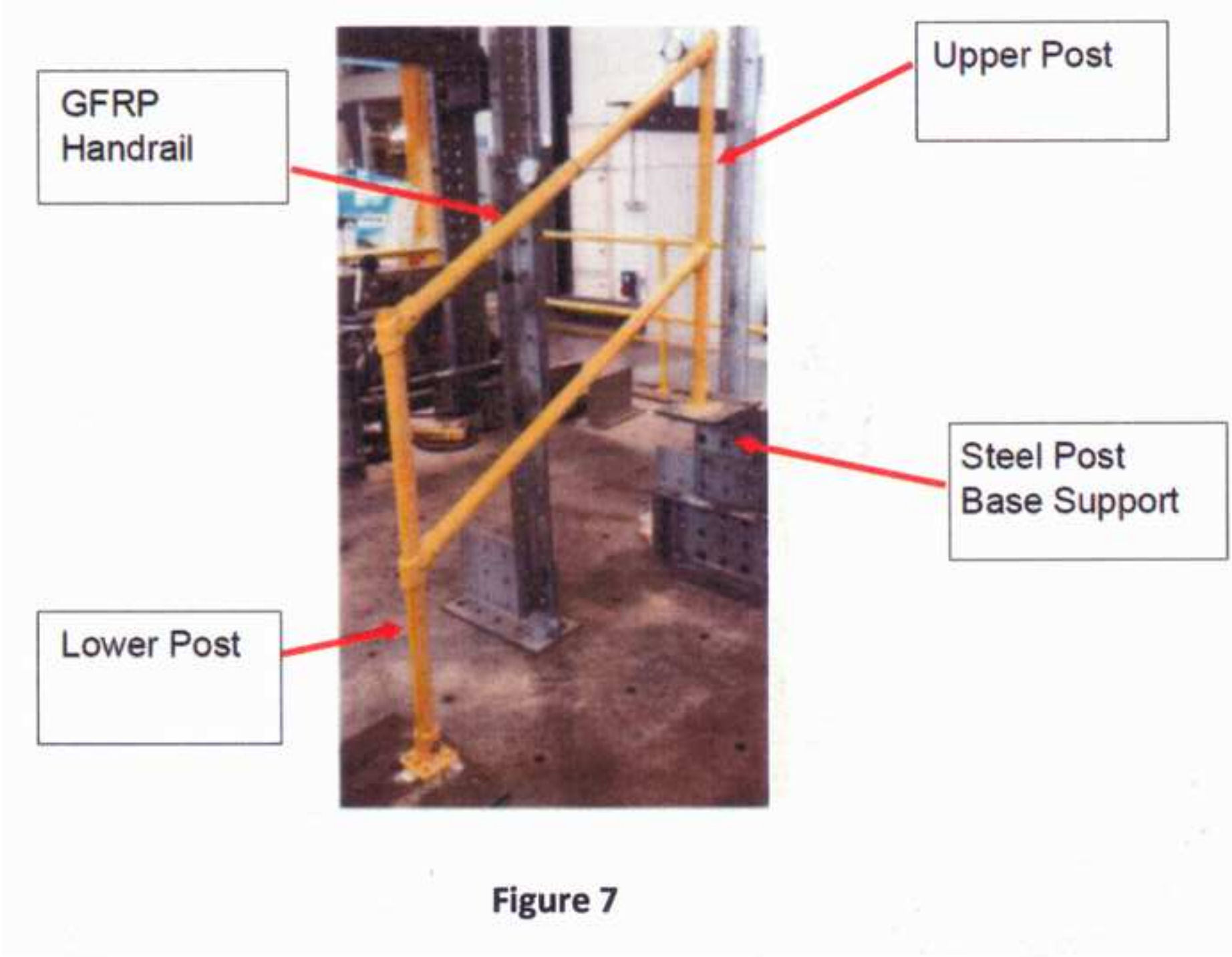

Figure 7

Figure 8

Click here to access/download;Figure;Figure 8 001.tif

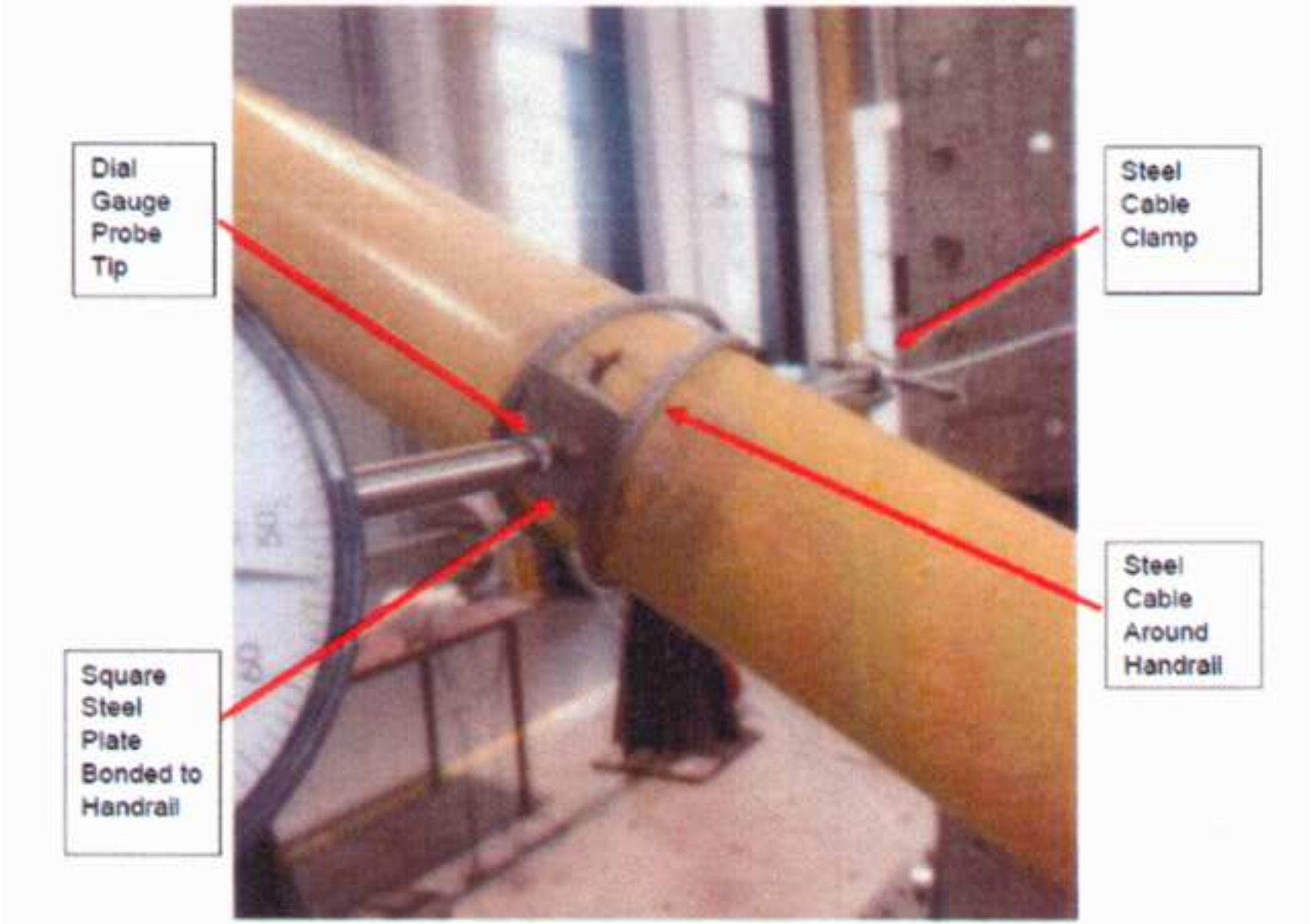

Figure 8

Figure 9

Click here to access/download;Figure;Figure 9 001.tif

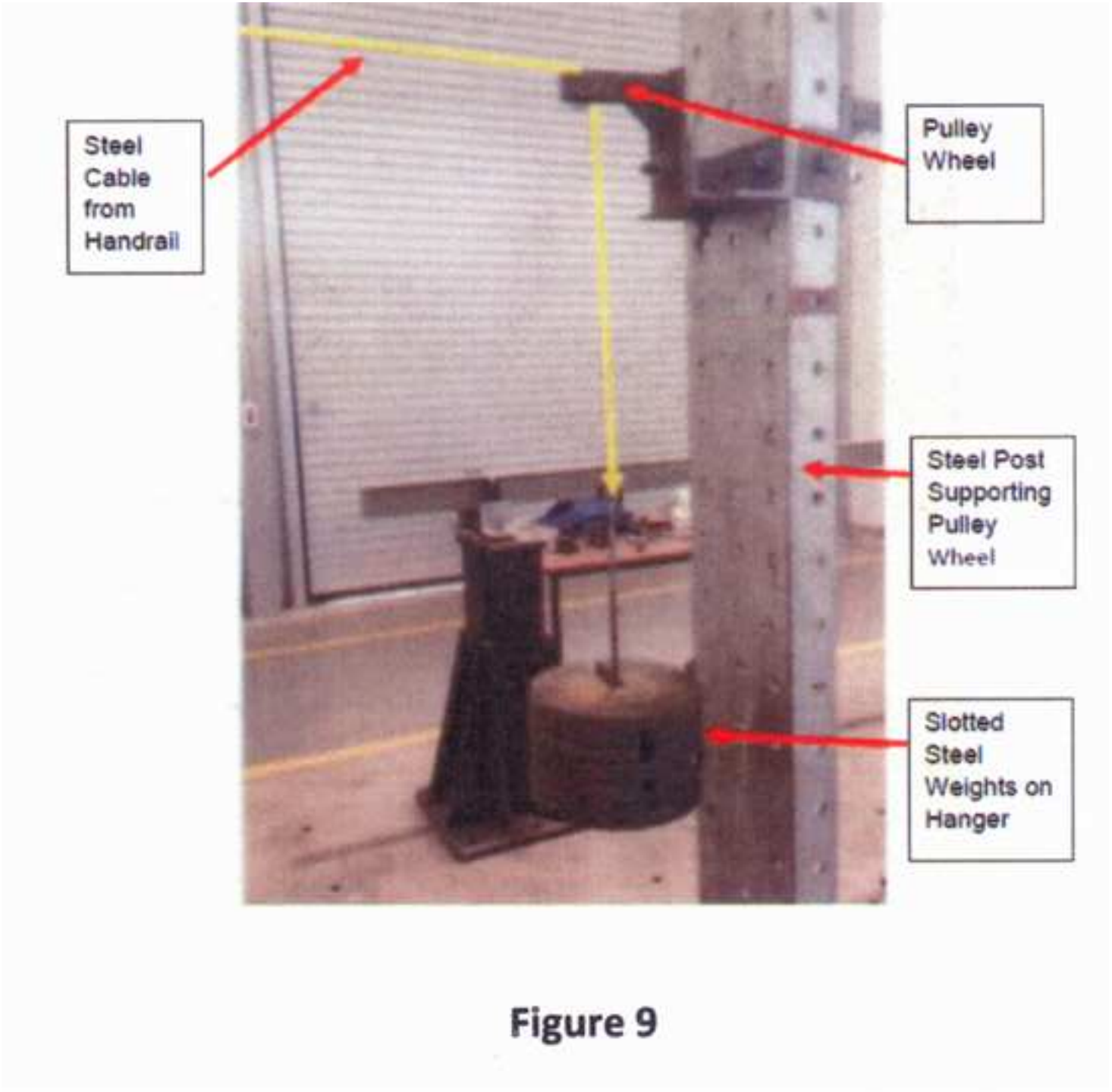

Figure 9

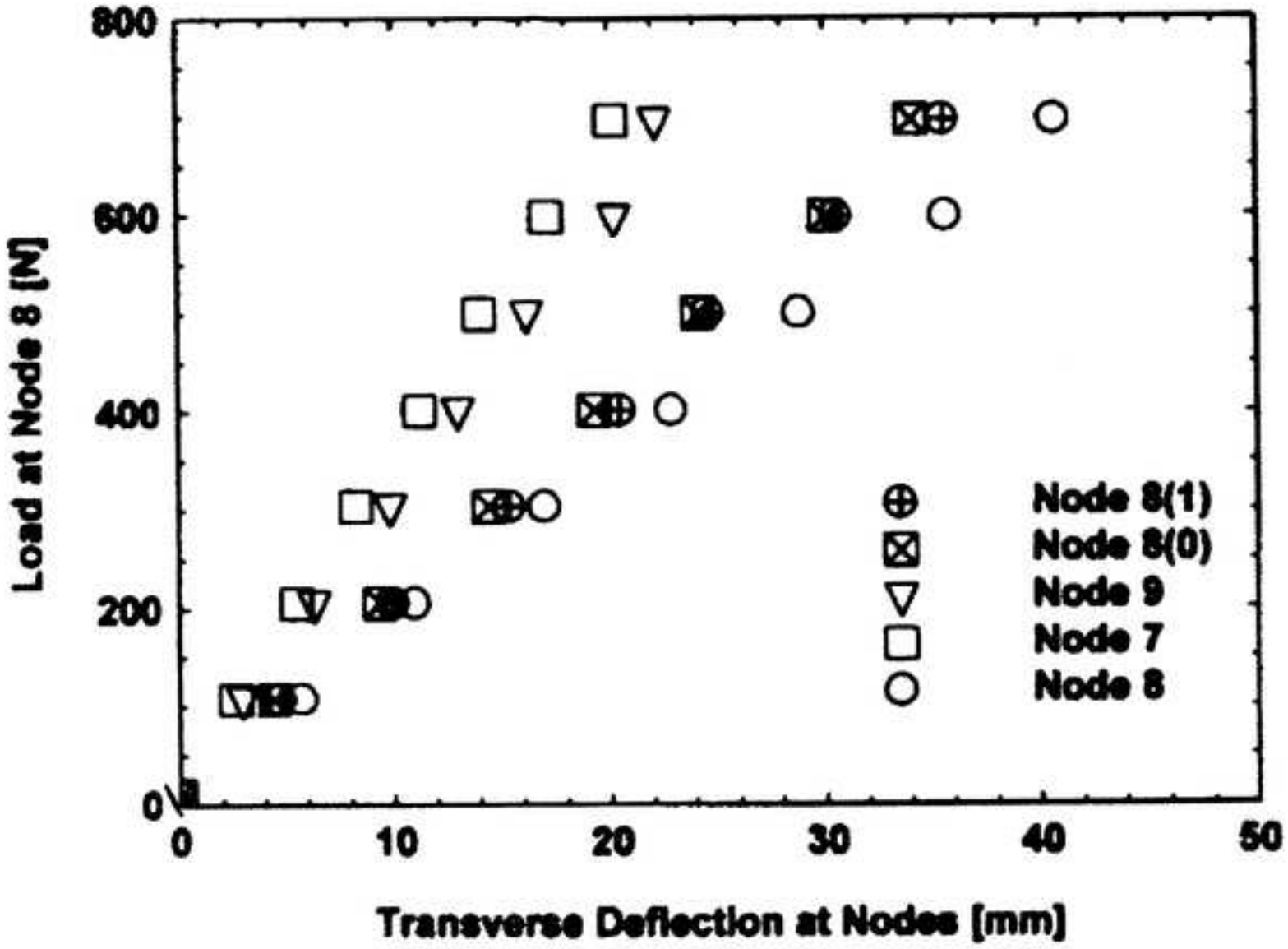

Figure 10

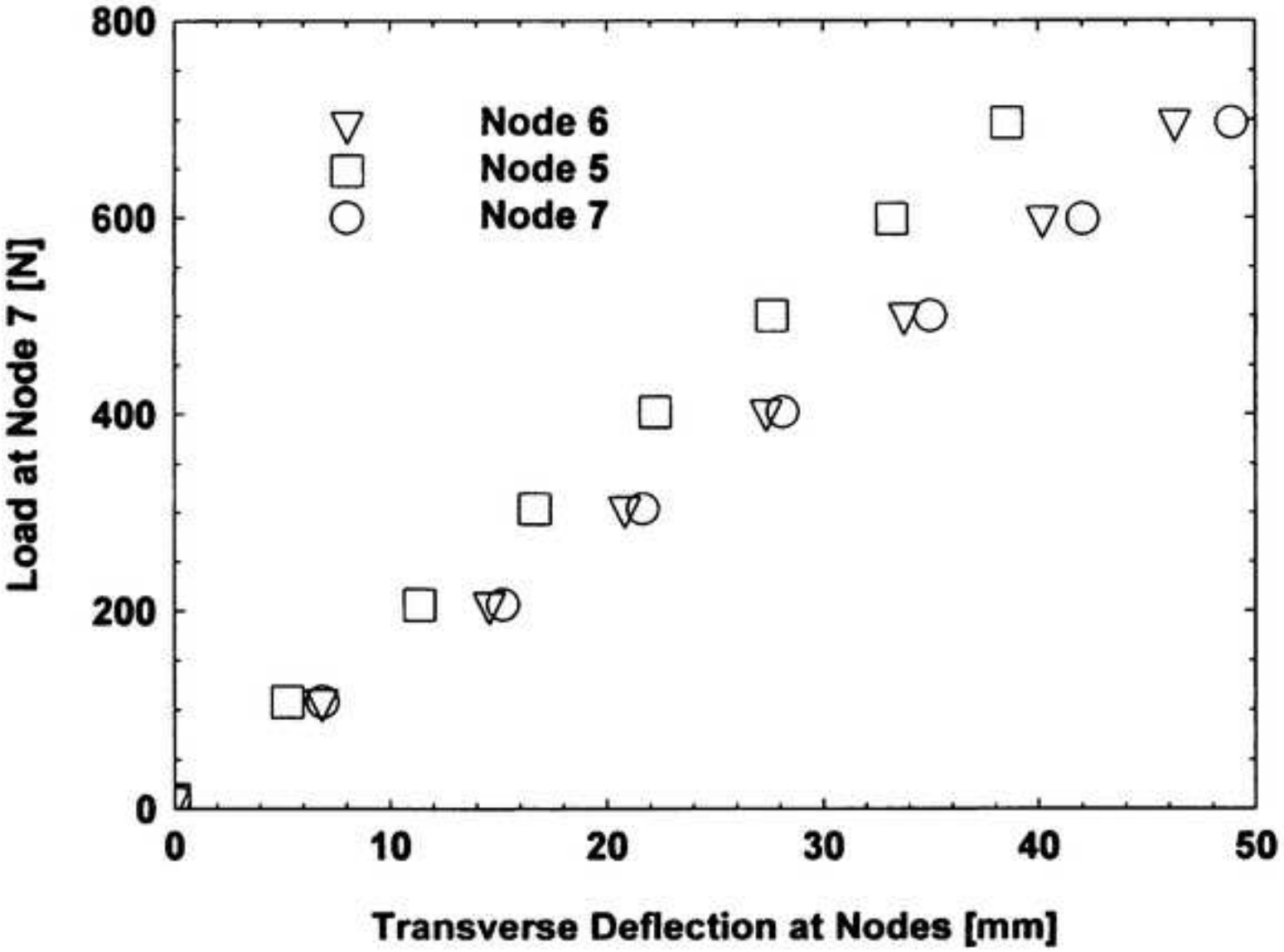

Figure 11

List of Figures and Captions

Figure 1: An overall view of an inclined two-bay guardrail showing the types and locations of the two-part bolted connectors forming the joints between the guardrails' tubes

Figure 2: Two-part bolted connectors: (a) two-way, (b) three-way and (c) four-way

Figure 3: (a) Foot base and (b) Side-fit base

Figure 4: Inclined single-bay guardrail

Figure 5: Inclined two-bay guardrail

Figure 6: Two-bay guardrail with a 30^o incline set up on the strong floor prior to testing

Figure 7: Single-bay guardrail with a 30^o incline and with its post bases bolted to the supports on the laboratory strong floor

Figure 8: Image of the cable attachment at the mid-bay of the handrail of a guardrail with a 30^o incline

Figure 9: Experimental setup for transferring the vertical load in the steel cable to a horizontal load applied at the mid-spans of the handrail or to the top of the centre-post of the two-bay 30^o inclined guardrail

Figure 10: Load versus deflection plots for the tops of the posts and the mid-spans of the handrails of the two-bay 30^o inclined guardrail

Figure 11: Load versus deflection plots for the tops of the posts and the mid-span of the handrail of the single-bay 30^o inclined guardrail

Table 1

Individual, mean and overall mean flexural moduli of the 800 mm and 1400 mm pultruded GFRP circular cross-section tubes

Tube Length [mm]	**Second Moment of Area [m^4x10^{-9}]**	**Reference Line**	**Mid-Span Load [N]**	**Mid-Span Deflection [mm]**	**Flexural Modulus [GPa]**	**Mean Flexural Modulus [GPa]**	**Overall Mean Flexural Modulus [GPa]**
800	181.13	A-A	488.88	1.00	28.79	28.54	31.34
		B-B	486.47		28.64		
		C-C	483.76		28.49		
		D-D	479.63		28.25		
1400		A-A	433.41	4.00	34.20	34.14	
		B-B	432.07		34.09		
		C-C	430.83		34.00		
		D-D	434.07		34.25		

Table 2

Individual, mean and overall mean shear moduli for the 200 mm, 400 mm and 600 mm pultruded GFRP circular cross-section tubes

Tube Length [mm]	**Test Number**	**Shear Modulus [GPa]**	**Mean Shear Modulus [GPa]**	**Overall Mean Shear Modulus [GPa]**
200	1	3.12	3.08	3.01
	2	2.97		
	3	3.16		
400	1	2.98	2.98	
	2	2.96		
	3	3.01		
600	1	2.91	2.96	
	2	2.88		
	3	3.08		

Table 3

Transverse nodal deflections of single-bay guardrails subjected to transverse loads of 697 N at the mid-span of the handrail and directed normal to the plane of the guardrail

Inclination Θ [degrees]	**Handrail Deflections [mm]**			**Mean Hand-Rail Deflection [mm]**	**Transverse Stiffness [kNm^{-1}]**
	Node 5	**Node 7**	**Node 6**		
0	27.55	**32.16**	27.55	29.09	24.0
15	27.04	**32.24**	27.42	28.90	24.1
30	25.97	**32.68**	26.27	28.31	24.6
45	24.40	**35.88**	23.06	27.78	25.1
60	23.28	**44.12**	14.80	27.40	25.4

Note: The bold values indicate the deflections of the loaded nodes.

Table 4

Transverse nodal deflections of two-bay guardrails subjected to transverse loads of 697 N applied in turn at the top of the centre post and at the mid-spans of the handrail and directed normal to the plane of the guardrail

Inclination Θ [degrees]	**Handrail Deflections [mm]**					**Mean Handrail Deflection [mm]**	**Transverse Stiffness [kNm^{-1}]**
	Node 7	**Node 8(0)**	**Node 8**	**Node 8(1)**	**Node 9**		
0	13.99	22.94	**27.23**	22.94	13.99	20.22	34.5
	27.18	**29.85**	22.94	13.94	5.14		
	5.14	13.94	22.94	**29.85**	27.18		
15	13.62	23.15	**27.88**	23.16	13.17	20.20	34.5
	26.90	**30.35**	23.15	13.69	4.21		
	4.70	13.68	23.16	**30.47**	27.26		
30	12.62	22.56	**27.94**	22.75	11.46	19.47	35.8
	25.03	**30.35**	22.56	12.98	3.62		
	4.74	12.98	22.75	**30.63**	25.54		
45	10.31	21.26	**28.36**	21.26	8.34	17.87	39.0
	22.84	**32.08**	21.26	11.02	2.09		
	3.63	11.01	22.36	**32.51**	22.16		
60	6.02	16.38	**29.54**	21.93	3.11	15.40	45.3
	20.92	**40.51**	16.40	5.49	0.78		
	1.09	5.43	21.86	**41.40**	14.36		

Note: The bold values indicate the deflections of the loaded nodes.

Table 5

Transverse nodal and mean deflections and transverse stiffnesses of the handrail of a single-bay guardrail with a 30^{o} incline

Load [N]	**Handrail Deflections [mm]**			**Mean Deflection [mm]**	**Transverse Stiffness [kNm^{-1}]**
	Node 5	**Node 7**	**Node 6**		
350	19.11	**25.20**	17.65	20.65	16.95
697	37.83	**50.02**	34.17	40.67	17.14

Note: The bold values indicate the deflections of the loaded nodes.

Table 6

Transverse nodal and mean deflections and transverse stiffnesses of the handrail of a two-bay guardrail with a 30^{o} incline

Load [N]	**Handrail Deflections [mm]**					**Mean Deflection [mm]**	**Transverse Stiffness [kNm^{-1}]**
	Node 7	**Node 8(0)**	**Node 8**	**Node 8(1)**	**Node 9**		
350	8.78	15.39	**21.12**	16.63	6.82	13.75	25.45
	17.39	**22.94**	15.41	8.90	2.56	13.44	26.04
	3.97	8.90	16.27	**23.14**	16.53	13.76	25.44
697	17.41	30.53	**41.74**	32.36	13.40	24.39	28.58
	34.60	**45.52**	30.72	17.70	5.16	26.74	26.07
	7.90	17.68	32.34	**46.31**	33.23	27.50	25.34

Note: The deflections in bold indicate the nodes at which the loads are applied.

Table 7

Comparison of numerical and experimental mean deflections and transverse stiffnesses of single-bay 30^{o} inclined guardrails subjected to approximate working loads of $350N$ at the mid-bay of the handrail

Numerical or Experimental Prediction	**Mean Deflection [mm]**	**Mean Transverse Stiffness [kNm^{-1}]**	**Percentage of Experimental Transverse Stiffness [%]**
ANSYS Workbench	20.65	16.95	108.8
Experiment	22.47	15.58	100

Table 8

Comparison of numerical and experimental mean deflections and transverse stiffnesses of two-bay 30^{o} inclined guardrails subjected to approximate working loads of $350N$ at the top of the centre post and the lower and upper mid-bays of the handrail

Numerical or Experimental Prediction	**Loaded Node of Handrail**	**Mean Handrail Deflection [mm]**	**Mean Transverse Stiffness [kNm^{-1}]**	**Percentage of Experimental Transverse Stiffness [%]**
ANSYS Workbench	Node 8	13.75	25.45	114.2
Experiment		15.70	22.29	100
ANSYS Workbench	Node 8(0)	13.44	26.04	116.67
Experiment		15.68	22.32	100
ANSYS Workbench	Node 8(1)	13.76	25.44	115.22
Experiment		15.86	22.07	100

Table 9

Comparison of numerical and experimental mean deflections and transverse stiffnesses of single-bay 30^o inclined guardrails subjected to the ultimate loads of $697N$ at the mid-bay of the handrail

Numerical or Experimental Prediction	**Mean Handrail Deflection [mm]**	**Mean Transverse Stiffness [kNm^{-1}]**	**Percentage of Experimental Transverse Stiffness [%]**
ANSYS Mechanical APDL	28.31	24.62	157.8
ANSYS Workbench	40.67	17.14	110.1
Experiment	44.68	15.60	100

Table 10

Comparison of numerical and experimental mean deflections and transverse stiffnesses of two-bay 30° inclined guardrails subjected to the ultimate loads of $697N$ at the top of the centre post and the lower and upper mid-bays of the handrail

Numerical or Experimental Prediction	**Loaded Node of Handrail**	**Mean Handrail Deflection [mm]**	**Mean Transverse Stiffness [kNm^{-1}]**	**Percentage of Experimental Transverse Stiffness [%]**
ANSYS Mechanical APDL	Node 8	19.47	35.81	159.0
ANSYS Workbench		27.07	25.75	114.3
Experiment		30.95	22.52	100
ANSYS Mechanical APDL	Node 8(0)	18.91	36.86	161.1
ANSYS Workbench		26.74	26.07	113.9
Experiment		30.47	22.88	100
ANSYS Mechanical APDL	Node 8(1)	19.33	36.06	160.0
ANSYS Workbench		27.49	25.35	112.5
Experiment		30.92	22.54	100

List of Tables, Titles and Footnotes

Table 1: Individual, mean and overall mean flexural moduli of the 800 mm and 1400 mm pultruded GFRP circular cross-section tubes

Table 2: Individual, mean and overall mean shear moduli for the 200 mm, 400 mm and 600 mm pultruded GFRP circular cross-section tubes

Table 3: Transverse nodal deflections of single-bay guardrails subjected to transverse loads of 697 N at the mid-span of the handrail and directed normal to the plane of the guardrail
Note: The bold values indicate the deflections of the loaded nodes.

Table 4: Transverse nodal deflections of two-bay guardrails subjected to transverse loads of 697 N applied in turn at the top of the centre post and at the mid-spans of the handrail and directed normal to the plane of the guardrail
Note: The bold values indicate the deflections of the loaded nodes

Table 5: Transverse nodal and mean deflections and transverse stiffnesses of the handrail of a single-bay guardrail with a 30^o incline
Note: The bold values indicate the deflections of the loaded nodes.

Table 6: Transverse nodal and mean deflections and transverse stiffnesses of the handrail of a two-bay guardrail with a 30^o incline
Note: The deflections in bold indicate the nodes at which the loads are applied.

Table 7: Comparison of numerical and experimental mean deflections and transverse stiffnesses of single-bay 30^o inclined guardrails subjected to approximate working loads of $350N$ at the mid-bay of the handrail

Table 8: Comparison of numerical and experimental mean deflections and transverse stiffnesses of two-bay 30^o inclined guardrails subjected to approximate working loads of $350N$ at the top of the centre post and the lower and upper mid-bays of the handrail

Table 9: Comparison of numerical and experimental mean deflections and transverse stiffnesses of single-bay 30^o inclined guardrails subjected to the ultimate loads of $697N$ at the mid-bay of the handrail

Table 10: Comparison of numerical and experimental mean deflections and transverse stiffnesses of two-bay 30^o inclined guardrails subjected to the ultimate loads of $697N$ at the top of the centre post and the lower and upper mid-bays of the handrail

Conflict of Interests Form. docx

Conflict of Interests Form

The Authors certify that they have no conflict of interests.

Please note: The Authors could not locate a Conflict of Interests Form on the website for the Composite Structures Journal, so they have uploaded this Word File instead.